

# Evolving marginal terranes during Neoproterozoic supercontinent reorganisation: constraints from the Bemarivo Belt in northern Madagascar

Sheree E. Armistead<sup>1\*</sup>, Alan S. Collins<sup>1</sup>, Justin L. Payne<sup>2</sup>, Grant M. Cox<sup>1</sup>, Andrew S. Merdith<sup>3</sup>, John D. Foden<sup>1</sup>, Théodore Razakamanana<sup>4</sup>, Bert De Waele<sup>5,6</sup>

<sup>1</sup>Centre for Tectonics, Resources and Exploration (TRaX), Department of Earth Sciences, The University of Adelaide, SA 5005, Australia

<sup>2</sup>Centre for Tectonics, Resources and Exploration (TraX), School of Built and Natural Environments, The University of South Australia, SA 5001, Australia

<sup>3</sup>LGL-TPE, Université Lyon 1, 69100, Villeurbanne, France

<sup>4</sup>Département des Sciences de la Terre, Université de Toliara, Toliara, Madagascar

<sup>5</sup>SRK Consulting, 10 Richardson Street, West Perth, WA 6005, Australia

<sup>6</sup>Department of Applied Geology, Curtin University, WA, Australia

Corresponding author: Sheree Armistead ([sheree.armistead@adelaide.edu.au](mailto:sheree.armistead@adelaide.edu.au))

## Key Points:

- New model linking northern Madagascar, Seychelles, NW India, Oman, south China at c. 750 Ma
- New zircon Hf and O isotope data from the Bemarivo Belt in northern Madagascar indicating that the northern Bemarivo Belt is juvenile
- Southern Bemarivo Belt has evolved Hf isotope signatures and likely links with central Madagascar magmatic suites

---

This manuscript is under review in TECTONICS.

Please note that subsequent versions of this manuscript will have slightly different content. If accepted, the final version of this manuscript will be available via the '*Peer-reviewed Publication DOI*' link on the right-hand side of this webpage. Please feel free to contact any of the authors, we welcome your feedback! 😊

---

## 1 Abstract

2 Madagascar is important for unravelling the geodynamic evolution of the transition between  
3 the Rodinia and Gondwana supercontinents as it contains several suites of c. 850–700 Ma  
4 magmatic rocks that have been postulated to correlate with other ex-Rodinia terranes. The  
5 Bemarivo Belt of northern Madagascar contains the youngest suite of these magmatic rocks  
6 that date to c. 750–700 Ma. We present zircon Hf and O isotope data from the Bemarivo Belt  
7 to understand its place in the Neoproterozoic plate tectonic reconfiguration. We demonstrate  
8 that the northern Bemarivo Belt is distinctly different from the southern Bemarivo Belt.  
9 Magmatic rocks of the southern Bemarivo Belt and Anaboriana Belt are characterised by  
10 evolved  $\epsilon_{\text{Hf}}(t)$  signatures and a range of  $\delta^{18}\text{O}$  values, similar to the Imorona-Itsindro Suite of  
11 central Madagascar. Magmatic rocks from the southern Bemarivo Belt, Anaboriana Belt and  
12 Imorona-Itsindro Suite likely formed together in the same long-lived volcanic arc. In contrast,  
13 the northern Bemarivo Belt contains juvenile  $\epsilon_{\text{Hf}}(t)$  and mantle-like  $\delta^{18}\text{O}$  values, with no  
14 probable link to the rest of Madagascar. We propose that the northern Bemarivo Belt formed  
15 in a juvenile arc system that included the Seychelles, Malani Igneous Suite of northwest India,  
16 Oman, and the Yangtze Belt of south China, outboard from continental India and south  
17 China. The final assembly of northern Madagascar and amalgamation of the northern and  
18 southern Bemarivo terranes occurred along the Antsaba subduction zone, with final assembly  
19 constrained by the c. 520 Ma post-tectonic Maevarano Suite.

## 20 1 Introduction

21 Reconstructing the tectonic geography of the ancient Earth and building a full-plate tectonic  
22 reconstruction for the globe in deep time is critically dependent on mapping the distribution  
23 of plate tectonic sensitive rocks through time (e.g. Merdith et al., 2017). A key goal is to  
24 understand the supercontinent cycle, and whether it operates as a simple pulse (e.g. Nance et  
25 al., 2014) or as a two-stage process starting with supercontinent initiation, followed by  
26 progressive accretion (e.g. Condie, 2002). This insight requires a detailed knowledge of the  
27 location and duration of the critical plate-margin geological events formed at either  
28 subduction zones or rifts (e.g. Mallard et al., 2016). The Neoproterozoic, in particular, is a  
29 critical period because it sees the major transition from the Nuna/Rodinia supercontinent  
30 cycle to the accretion and amalgamation of Gondwana/Pangaea (Merdith et al., 2018). Much  
31 of the evidence for this billion-year timescale plate reconfiguration is found in the East African  
32 Orogen that formed as the Mozambique Ocean closed and Neoproterozoic India collided with  
33 the Congo Craton to form central Gondwana (Armistead et al., 2017; Collins and Pisarevsky,

34 2005; Fritz et al., 2013). Madagascar was located in the centre of the East African Orogen and  
35 provides an ideal natural laboratory to study how the active margins that consumed the  
36 Mozambique Ocean evolved to form the supercontinent Gondwana. Of particular interest and  
37 contention, is how and when the Archean nucleus of Madagascar amalgamated with the  
38 Dharwar Craton of India to the east, and East Africa to the west, as well as with smaller  
39 continental blocks of equivocal origin. One of these blocks—the Bemarivo Belt of northern  
40 Madagascar—is composed of Neoproterozoic rocks spanning c. 750–700 Ma. Its evolution and  
41 amalgamation with the rest of Madagascar is poorly understood and is the focus of this study.

42 Madagascar is made up of several terranes spanning from Archean to recent times. The centre  
43 of Madagascar is made up of the Antananarivo Craton, which is composed of c. 2500 Ma  
44 magmatic gneisses (Collins and Windley, 2002; Kröner et al., 2000). To the east of this craton  
45 are the Antongil and Masora cratons. These contain rocks that are c. 3100 Ma and are likely a  
46 continuation of the Dharwar Craton of India (Armistead et al., 2017; Schofield et al., 2010;  
47 Tucker et al., 1999b). To the southwest of the Antananarivo Craton is the Itremo Group, made  
48 up of quartzites, schists and marbles with a maximum depositional age of c. 1600 Ma (Cox et  
49 al., 1998; Fernandez et al., 2003). To the southwest of this, is the Ikalamavony Group,  
50 similarly made up of quartzites, schists and marbles, but with a maximum depositional age of  
51 c. 1000 Ma. To the south of these metasedimentary sequences are the Proterozoic Anosyén,  
52 Androyén and Vohibory terranes (Boger et al., 2014; Emmel et al., 2008; Jöns and Schenk,  
53 2007).

54 North of the Antananarivo Craton is the Bemarivo Belt, made up of the Paleoproterozoic  
55 Sahantaha Group, and intruded by c. 750–700 Ma magmatic rocks with a range of  
56 geochemical compositions (Thomas et al., 2009). Separating the Antananarivo Craton from  
57 the Bemarivo Belt, is the Anaboriana-Manampotsy belt—an interpreted late Neoproterozoic  
58 sequence of gneisses thought to represent the suture between Madagascar and the Dharwar  
59 Craton of India (Collins and Windley, 2002).

60 Northern Madagascar comprises the c. 3100 Ma Antongil Craton, the c. 2500 Ma  
61 Antananarivo Craton and the c. 750–700 Ma Bemarivo Belt (Figure 1), all of which have  
62 debatable geological histories. It is well documented that the Antongil Craton of northern  
63 Madagascar shares many characteristics with the Dharwar Craton of India, and that these two  
64 terranes were probably contiguous until the breakup of Gondwana (Armistead et al., 2017;  
65 Bauer et al., 2011; Collins and Windley, 2002; Schofield et al., 2010). However, the timing of  
66 collision between the Antongil-Dharwar Craton of India and the rest of Madagascar is a

67 contentious topic. Two end-member models are generally evaluated for the amalgamation of  
68 Madagascar; 1) the Antongil(Dharwar)-Madagascar collision occurred in the late Archean, and  
69 central Madagascar and the Dharwar Craton have existed as “the Greater Dharwar Craton”  
70 from then until the breakup of Gondwana (Tucker et al., 2011); or 2) Antongil(Dharwar) and  
71 central Madagascar were separate terranes that were sutured during the major Ediacaran–  
72 Cambrian Malagasy Orogeny, marked by the Betsimisaraka Suture (Collins and Windley,  
73 2002). Understanding the timing and nature of the assembly of northern Madagascar will  
74 provide important constraints on the amalgamation of Madagascar more broadly.

### 75 **1.1 Regional Geology of the Bemarivo Belt**

76 A World Bank Project in Madagascar led to the collection of a substantial dataset of  
77 geochemical, geochronological and stratigraphic data from northern Madagascar (BGS-USGS-  
78 GLW, 2008). The Bemarivo Belt has loosely been divided into two terranes separated by the  
79 ~east–west trending Antsaba Shear Zone (Figure 1)(Thomas et al., 2009).

80 The southern Bemarivo Belt contains the Sahantaha Group, a metasedimentary sequence  
81 derived from Paleoproterozoic sources. This sequence has been interpreted as the passive  
82 margin sequence to the Antananarivo Craton. The Sahantaha Group contains similar rock  
83 types, and detrital zircons with similar dates to the Itremo Group of central Madagascar (BGS-  
84 USGS-GLW, 2008; Cox et al., 1998; Cox et al., 2004; De Waele et al., 2011; Fitzsimons and  
85 Hulscher, 2005). The Sahantaha Group is intruded by the c. 750 Ma Antsirabe Nord Suite, a  
86 plutonic suite ranging from gabbro to granite (Thomas et al., 2009).

87 The northern Bemarivo Belt contains a component of metamorphosed Archean schist and  
88 gneiss—the c. 2477 Ma Betsiaka Group, although outcrops of these rocks are scarce and  
89 geographically restricted to the northwest margin of the Bemarivo Belt (Thomas et al., 2009).  
90 The Betsiaka Group is in fault-contact with the northern Bemarivo units and possibly  
91 represents a faulted block of the Antananarivo Domain. Two volcano-sedimentary groups  
92 were deposited in the northern Bemarivo Belt at c. 750–720 Ma. The high-grade, amphibolite-  
93 facies volcano-sedimentary Milanao Group has a maximum depositional age of c. 750 Ma, and  
94 the low-grade, greenschist to lower amphibolite facies, Daraina Group has an extrusive age of  
95 c. 740–730 Ma (Thomas et al., 2009). These groups are intruded by arc-related rocks of the  
96 Manambato Suite, which comprises c. 718–705 Ma magmatic rocks (Thomas et al., 2009).

97 Much of northern Madagascar is intruded by the c. 530 Ma Maevarano Suite, interpreted as  
98 post-tectonic granites that formed due to orogenic collapse of the East African Orogen

99 (Goodenough et al., 2010). This suite has been used as a maximum age constraint on the final  
100 assembly of northern Madagascar, based on the interpretation that it is exposed in all terranes  
101 of northern Madagascar (Goodenough et al., 2010; Thomas et al., 2009).

102 When considered as a single coherent terrane, the northern and southern Bemarivo belts have  
103 been interpreted as a juvenile arc terrane that was accreted to the Antananarivo Craton along  
104 a Neoproterozoic–Cambrian suture (Thomas et al., 2009). Juvenile Nd data was reported in  
105 abstract only (Tucker et al., 1999a) and has been used as evidence for the juvenile nature of  
106 both the northern and southern Bemarivo belts. However, sample locations were not reported  
107 and it remains unclear whether these samples were collected from the northern or southern  
108 Bemarivo Belt. Extensive whole-rock geochemistry data collected through the World Bank  
109 Project (BGS-USGS-GLW, 2008; Thomas et al., 2009) suggest that much of the Bemarivo Belt  
110 formed from volcanic arc processes. This interpretation was based on Y-Nb tectonic  
111 discrimination diagrams, and the calc-alkaline nature of the rocks preserved in the Bemarivo  
112 Belt. However, a lack of published isotopic data beyond zircon U–Pb geochronology for this  
113 region limits our ability to fully understand the magma processes and crustal assimilation  
114 involved in the evolution of the Bemarivo Belt. Understanding the isotopic nature of these  
115 magmatic suites in terms of their crustal versus mantle components, is important for  
116 correlating them with other age-equivalent terranes. The age-equivalent c. 850–750 Ma  
117 Imorona-Itsindro magmatic suite is widespread in central Madagascar (Archibald et al., 2016;  
118 Archibald et al., 2017b; Zhou et al., 2018), and may form a continuum with the Bemarivo Belt.  
119 Likewise, there are age-equivalent terranes in the Seychelles, the Malani Igneous Suite of  
120 northwest India and the Yangtze Belt of south China. However, isotopic data, in addition to  
121 conventional U–Pb zircon dating is needed to test the robustness of these correlations. We  
122 have collected Hf and O isotope data from zircon within the Bemarivo Belt of northern  
123 Madagascar to characterise the evolution of this terrane and compare it to terranes elsewhere  
124 in Madagascar and globally. Integrating this dataset within a plate tectonic framework using  
125 GPlates reconstruction software, allows us to assess tectonic models both temporally and  
126 spatially. The results of this study are important for supercontinent reconstructions of both  
127 Rodinia and Gondwana.

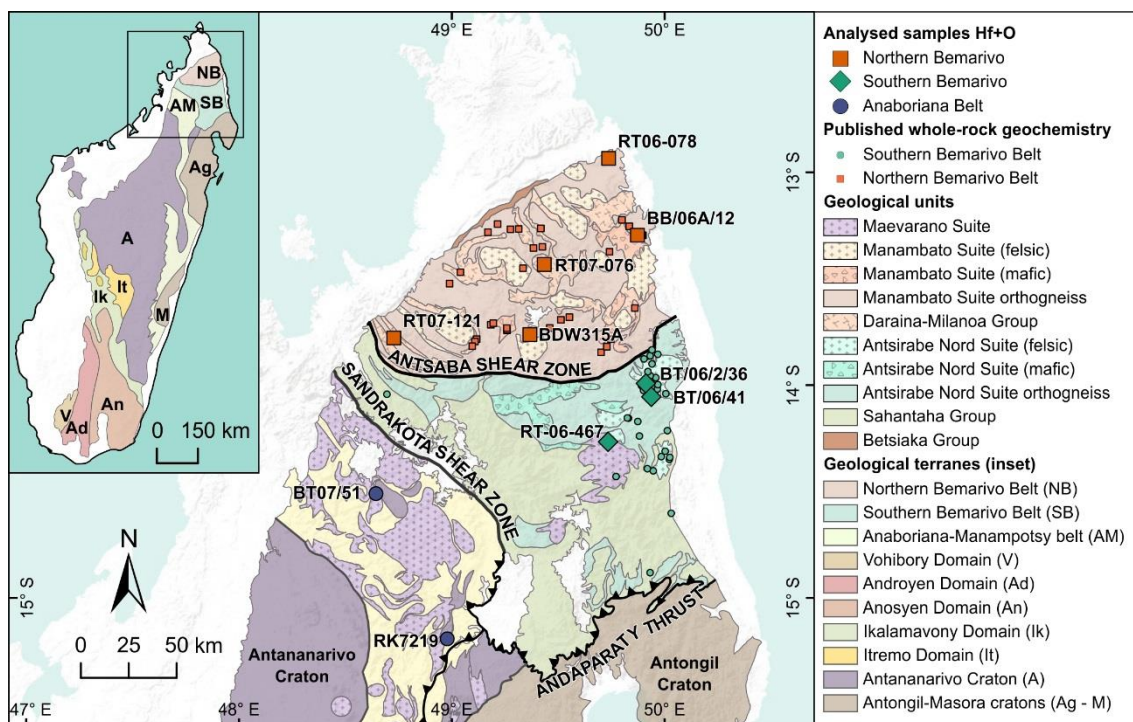


Figure 1 Geological map of northern Madagascar modified to reflect our interpretation of the region. Modified from Roig et al. (2012) and Thomas et al. (2009), inset modified from De Waele et al. (2011).

## 2 Methodology

Zircon grains were selected from those analysed for U–Pb through the Madagascar World Bank Project (BGS-USGS-GLW, 2008). Ten samples that cover a broad area in northern Madagascar were selected for Hf and O analysis to characterise the isotopic nature of this region (Figure 1). Detailed methodologies are provided in Supplementary file A and isotopic data are provided in Supplementary file B. Zircon U–Pb data were collected using the SHRIMP instrument at the John de Laeter Research Centre at Curtin University (BGS-USGS-GLW, 2008; Thomas et al., 2009). We have reinterpreted weighted averages from these data for consistency and these are summarised in Table 1.

## 3 Zircon U–Pb, Hf and O isotope data

### 3.1 Anaboriana Belt

Two gneiss samples (BT0751 and RK7219) analysed from the Anaboriana Belt have ambiguous protoliths and it is unclear if they are derived from magmatic or sedimentary protoliths (BGS-USGS-GLW, 2008). U–Pb geochronology was unable to resolve this as there is considerable scatter on concordia plots for both samples, which could be either lead loss due to metamorphism or a detrital array.  $^{176}\text{Hf}/^{177}\text{Hf}_i$  values obtained for these samples are

147 consistent with lead loss and age resetting for the zircon grains as the values plot in a  
148 horizontal array (within uncertainty) across an age vs.  $^{176}\text{Hf}/^{177}\text{Hf}_i$  plot. Although the Hf  
149 isotope data are not conclusive, a magmatic protolith is also supported by the O isotope  
150 values. Analyses from the two samples have  $\delta^{18}\text{O}$  values between +1.3 ‰ and +4.4 ‰. These  
151 values are below values normally expected for crustal or mantle values and are typically  
152 associated with the involvement of meteoric waters being involved in hydrothermal alteration  
153 of volcanic/sub-volcanic magma systems (e.g. Bindeman and Valley, 2001; Valley et al., 1998).  
154 It is highly unlikely that anomalous values such as these could be recorded in every single  
155 magma system that contributed detritus to a sedimentary rocks, and hence the samples are  
156 considered to have igneous protoliths—potentially volcanic or upper crustal intrusives.

157 Calculated magmatic crystallisation ages for samples RK7219 and BT0751 are  $750 \pm 4$  Ma and  
158  $768 \pm 8$  Ma ( $2\sigma$ ) respectively (Table 1). When calculated at these ages (to remove the effects of  
159 Pb-loss),  $\epsilon_{\text{Hf}}(t)$  values for magmatic zircons are in the range -3.4 to -10.1. Four U–Pb rim  
160 analyses from sample RK7219 yield a calculated age of  $514 \pm 6$  Ma and seven analyses from  
161 sample BT0751 yield an age of  $518 \pm 4$  Ma, which we interpret as the age of metamorphism.

### 162 3.2 Southern Bemarivo

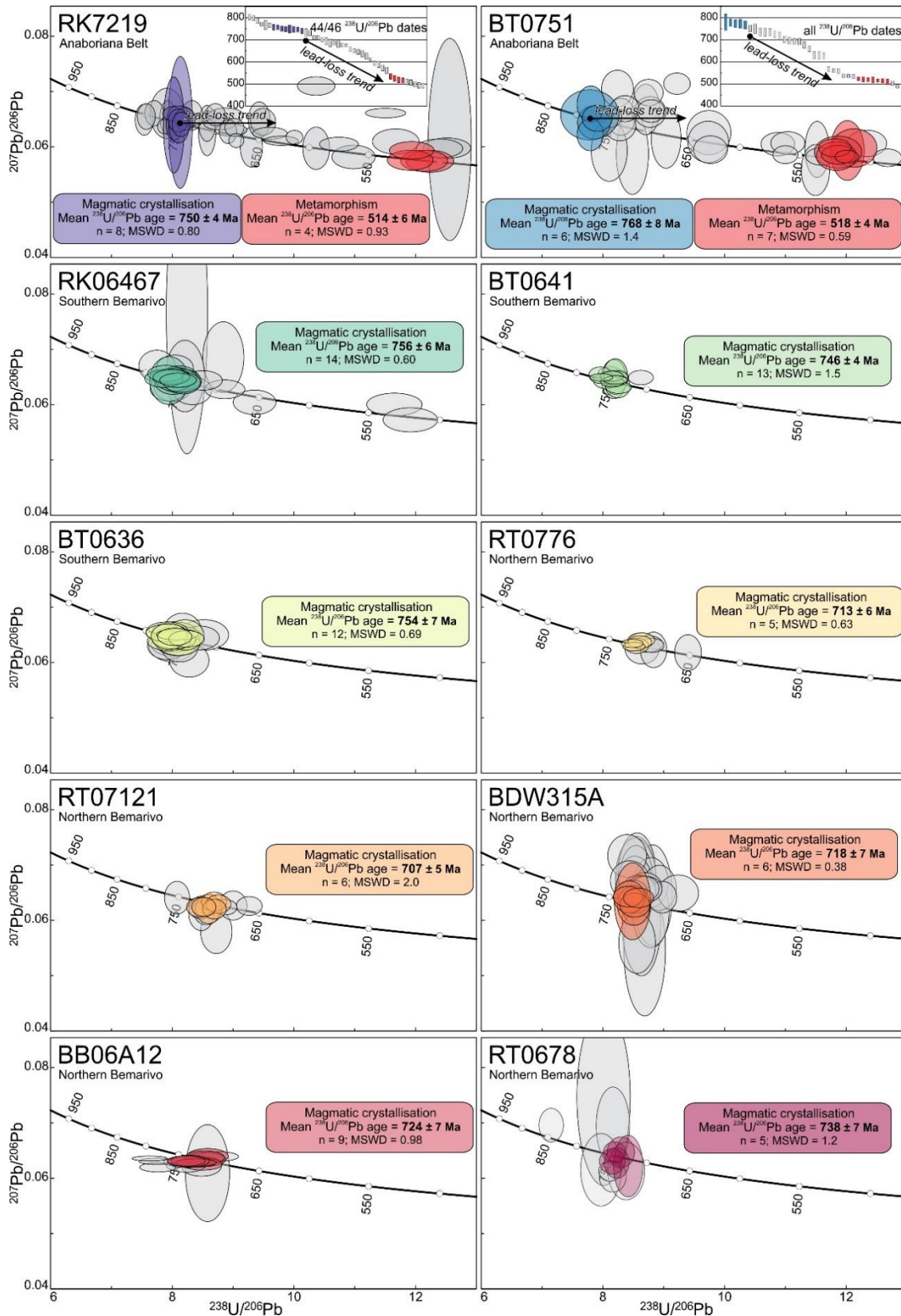
163 Three samples were analysed from the southern Bemarivo Belt. These rocks include,  
164 granodioritic gneiss, tonalitic gneiss and diorite (Table 1). Interpreted magmatic  
165 crystallisation ages for these rocks range from c. 756 Ma to c. 746 Ma (Figure 2). Lu–Hf  
166 analyses from samples BT0636, BT0641 and RT06467 have negative  $\epsilon_{\text{Hf}}(t)$  values ranging from  
167 -15.0 to -1.5 (Figure 3). These analyses have two-stage depleted mantle model ages spanning  
168 c. 2.6–1.7 Ga.

169 Oxygen isotope data from the southern Bemarivo Belt show a wide range of  $\delta^{18}\text{O}$  values. The  
170 majority of analyses from samples BT0641 and BT0636 are between +4.8 ‰ and +5.9 ‰,  
171 overlapping with the range of values expected for mantle-derived zircons, but extending to  
172 more positive values consistent with samples that have crystallised in equilibrium with  
173 surface-derived water (Valley et al., 1998). Four analyses from sample BT0641 and two  
174 analyses from sample BT0636 have  $\delta^{18}\text{O}$  values lower than what is expected for mantle  
175 sources, ranging from +0.6 ‰ to +4.3 ‰. The majority of analyses from sample RT06467 are  
176 between +6.3 ‰ and +7.1 ‰, with two analyses of +5.8 ‰ that overlap with the mantle  $\delta^{18}\text{O}$   
177 field.

178 **3.3 Northern Bemarivo**

179 Five samples from the northern Bemarivo Belt were used for Hf and O isotopic analysis on  
180 zircon. These rocks include, granites, granodioritic gneisses and rhyolites (Table 1). Magmatic  
181 crystallisation ages for these samples are younger than for the southern Bemarivo Belt and  
182 range from c. 740 Ma to c. 705 Ma. Lu–Hf analyses from northern Bemarivo samples cluster to  
183 form a group of similar  $\epsilon_{\text{Hf}}(t)$  signature and age. These analyses have positive  $\epsilon_{\text{Hf}}(t)$  values  
184 between +4 and +11 and depleted mantle model ages spanning c. 1.4–1.0 Ga (Figure 3).

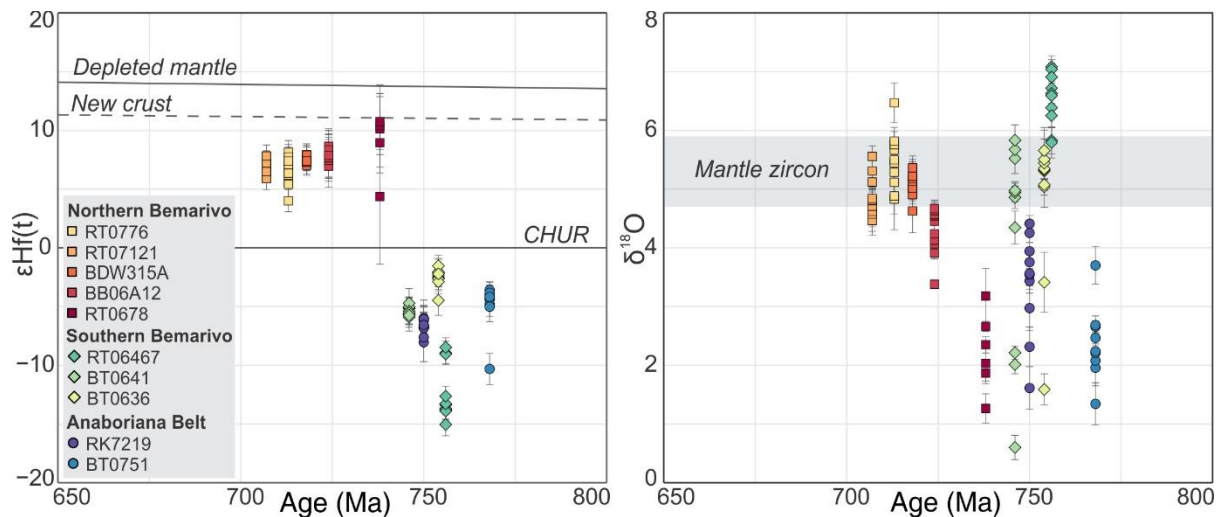
185 Samples from the northern Bemarivo Belt preserve a restricted range of  $\delta^{18}\text{O}$  values. Analyses  
186 from samples RT0776, RT07121 and BDW315A have  $\delta^{18}\text{O}$  values ranging from +4.4 ‰ to  
187 +6.5 ‰ (Figure 3). These overlap with the range of values typical for mantle-derived zircons  
188 ( $5.3 \pm 0.6$  ‰; Valley et al. (1998)). Samples BB06A12 and RT06-78 have lower  $\delta^{18}\text{O}$  values,  
189 with mean  $\delta^{18}\text{O}$  values of +4.3 ‰ and +2.3 ‰ respectively.



190

191 Figure 2 Concordia plots with reinterpreted ages using data from Thomas et al. (2009). Axes are the same  
 192 range for all plots. Coloured ellipses were used to calculate the ages provided, grey ellipses show remaining  
 193 data that were excluded from calculations.

194



195

196

197

198

199

Figure 3  $\epsilon_{\text{Hf}}(t)$  vs Age and  $\delta^{18}\text{O}$  vs Age (calculated  $^{238}\text{U}/^{206}\text{Pb}$  magmatic crystallisation ages) for samples analysed from northern Madagascar.  $\epsilon_{\text{Hf}}(t)$  for each analysis was calculated using the magmatic crystallisation age, data given in Supplementary file B. Plots produced in R, code written to produce plots is documented in supplementary file C.

200

#### 4 Insights from published whole-rock geochemistry data

201

202

203

204

205

206

207

208

209

210

211

212

Whole-rock geochemistry from the northern and southern Bemarivo Belt was published in Thomas et al. (2009). We have used these data to further compare and contrast the northern and southern Bemarivo Belts. We have shown that magmatic rocks from the southern Bemarivo Belt have evolved  $\epsilon_{\text{Hf}}(t)$  signatures, so the geochemistry is potentially more reflective of the crust that's being incorporated rather than the processes that generated the mantle melts. Although there are only three samples that have both Hf isotope and whole-rock geochemistry data for the southern Bemarivo Belt, there does appear to be a trend between these two datasets. The more evolved sample has a more ferroan signature than the less evolved sample, which has a magnesian signature (Figure 4a). There is an increase in alkalinity for increasing  $\epsilon_{\text{Hf}}(t)$  values (Figure 4b). The Sr anomalies and trace elements are also higher for the more evolved samples (Figure 4d, e). Together, this suggests that crustal assimilation was the dominant cause for changing  $\epsilon_{\text{Hf}}(t)$ .

213

214

215

216

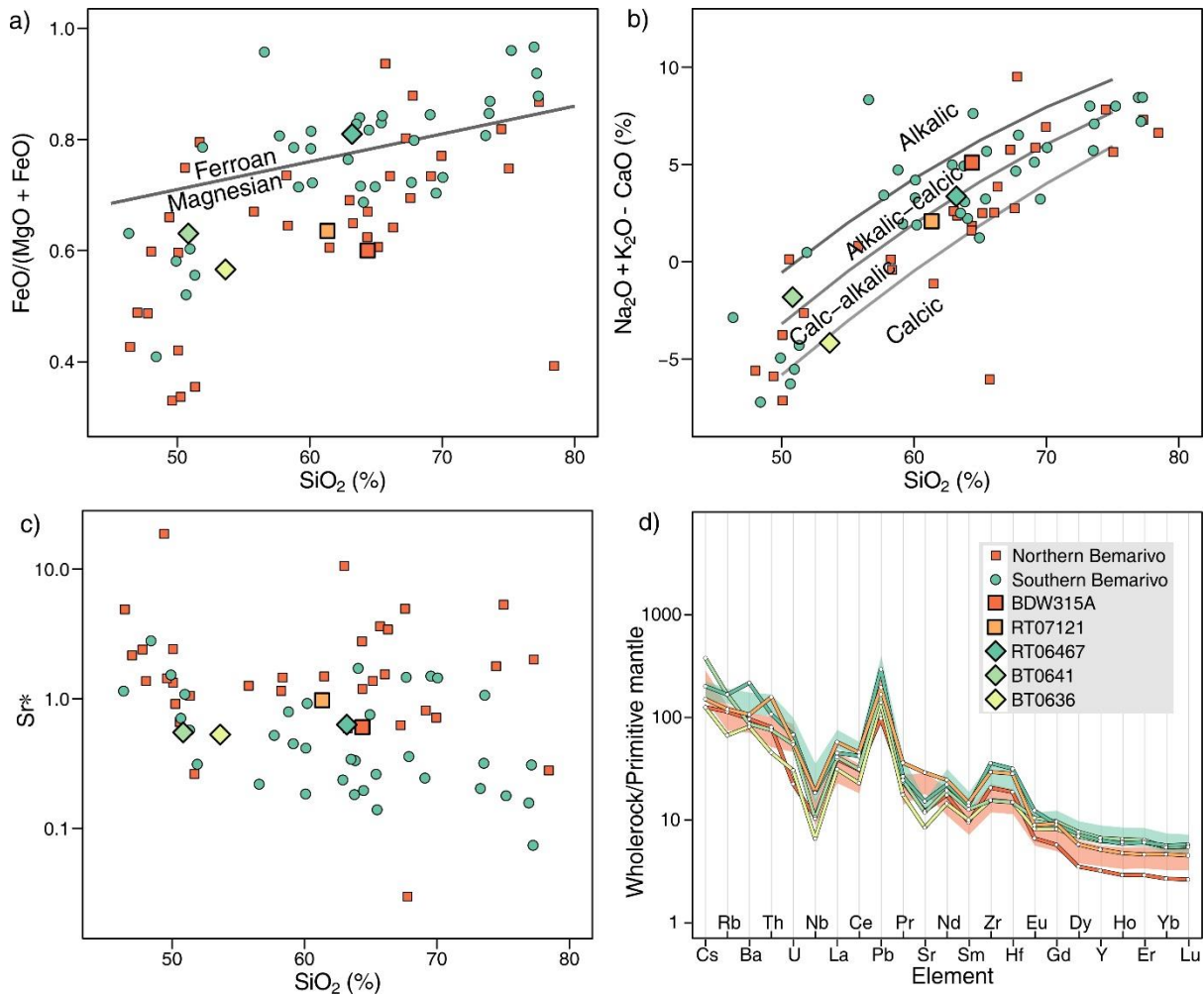
217

218

219

In contrast, samples from the northern Bemarivo Belt are dominantly magnesian (Figure 4a), calc-alkalic (Figure 4b), and are not as enriched in trace elements (Figure 4e). Combined with the juvenile nature of these rocks, we suggest they most likely formed in an arc environment, consistent with the interpretation of Thomas et al. (2009). Although there are only two samples with both Hf isotope and geochemistry data, the younger, slightly more evolved sample has a higher Sr anomaly and higher values for the majority of the trace elements (Figure 4c, d). This suggests that low degrees of fractionation and crustal

220 assimilation may have been involved in the evolution of the northern Bemarivo Belt, which  
 221 accounts for the trend of decreasing  $\epsilon_{\text{Hf}}(t)$  values with time (Figure 3).



222  
 223 Figure 4 a) Fields for ferroan and magnesian rocks after Frost and Frost (2008); b) fields for alkali, alkali-calcic,  
 224 calc-alkaline and calcic after Frost and Frost (2008); c) Sr anomaly ( $Sr^*$ ) calculated as  $Sr_N/\sqrt{Pr_N \cdot Nd_N}$ ,  
 225 where N is the chondrite normalised values after Sun and McDonough (1989); and d) Spider plot for samples  
 226 with Hf and O isotope data. The shaded bands behind these lines are the bootstrapped mean and 95%  
 227 confidence intervals of Primitive Mantle normalised elemental data for all samples from the northern and  
 228 southern Bemarivo belts; normalising values from Sun and McDonough (1989). Bootstrapping was performed  
 229 with replacement for 50000 repetitions. R scripts to produce plots are provided in supplementary file C. Data  
 230 from Thomas et al. (2009).

## 231 5 Regional evolution of the Bemarivo Belt

232 The Bemarivo Belt of northern Madagascar has previously been interpreted as a juvenile  
 233 Neoproterozoic arc-related terrane that amalgamated with the central Madagascar craton in  
 234 the late Neoproterozoic to early Cambrian (Collins, 2006; Kröner et al., 2000; Tucker et al.,  
 235 1999a). Possible genetic links between Madagascar and the Seychelles, Malani Igneous Suite  
 236 of northwest India and south China have been proposed (Ashwal et al., 2002; Tucker et al.,

237 1999a; Wang et al., 2017). New Hf and O isotope data collected in this study allow us to  
238 interpret the tectonic evolution of the Bemarivo Belt and assess possible paleogeographical  
239 links. Distinct differences between these terranes indicate that they have undergone different  
240 tectonic histories at different times during the Neoproterozoic.

### 241 **5.1 Anaboriana Belt**

242 Zircons analysed from the two Anaboriana Belt samples have evolved  $\epsilon_{\text{Hf}}(t)$  signatures that  
243 overlap with values from southern Bemarivo Belt samples, but are generally less evolved than  
244 those from the slightly older Imorona-Itsindro Suite (Archibald et al., 2016; Zhou et al., 2018).  
245 We interpret this evolved signature as the result of incorporation of crustal material during  
246 magma genesis.  $\delta^{18}\text{O}$  values for the Anaboriana Belt samples are lower than most analyses  
247 from the southern Bemarivo Belt. Low  $\delta^{18}\text{O}$  values are typically the result of hydrothermal  
248 cycling of meteoric water during magma generation (Bindeman and Valley, 2001; Valley et al.,  
249 1998). These are often correlated with extensional environments where rifting may have  
250 occurred that facilitated hydrothermal circulation in near-surface or volcanic settings  
251 (Bindeman and Valley, 2001; Valley et al., 1998). We therefore suggest that the Anaboriana  
252 Belt samples were generated from magmas that contained a component of older crustal  
253 material, but likely underwent hydrothermal alteration in an extensional environment.

### 254 **5.2 Southern Bemarivo Belt**

255 The southern Bemarivo Belt samples contain zircons with negative  $\epsilon_{\text{Hf}}(t)$  signatures that  
256 suggest a contribution of continental crust during magma generation.  $\epsilon_{\text{Hf}}(t)$  model ages for  
257 these analyses range between c. 2.56–1.73 Ga. The majority of  $\delta^{18}\text{O}$  analyses from sample  
258 BT06467 are above the mantle range, indicating that supra-crustal rock assimilation and  
259 melting were involved in magma generation. The majority of zircon analyses from samples  
260 BT0641 and BT0636 have  $\delta^{18}\text{O}$  values in the mantle range. Several analyses from the  
261 aforementioned samples, as well as analyses from the Anaboriana Belt samples RK7219 and  
262 BT0751, have very low  $\delta^{18}\text{O}$  values that suggest the involvement of meteoric fluids and  
263 hydrothermal alteration in a similar way to that envisaged for similar values from the Tonian  
264 Imorona-Itsindro Suite in central Madagascar by Archibald et al. (2016).

265 The Sahantaha Group in which these magmatic rocks intrude, have major detrital zircon  
266 components of c. 2500–1700 Ma (De Waele et al., 2011), broadly overlapping with the range  
267 of depleted mantle model ages for the analysed samples. The Antananarivo Domain, which  
268 may underlie the Sahantaha Group, is dominantly comprised of c. 2500 Ma gneisses. The data  
269 presented here support the interpretation of Thomas et al. (2009) that subduction was taking

270 place beneath the Sahantaha Group (and underlying Antananarivo Domain) at c. 750 Ma,  
271 which produced melts that incorporated crustal material from surrounding rocks. This  
272 interpretation is consistent with previous models for the southern Bemarivo Belt (Thomas et  
273 al., 2009). Low  $\delta^{18}\text{O}$  samples from the Anaboriana Belt may have formed in a back-arc  
274 extensional environment to the main southern Bemarivo volcanic arc.

### 275 **5.3 Northern Bemarivo Belt**

276 Samples analysed from the northern Bemarivo Belt are dominated by relatively juvenile  $\epsilon_{\text{Hf}}(t)$   
277 signatures, and  $\delta^{18}\text{O}$  values that suggest a mantle source and relatively little assimilation of  
278 supra-crustal material. The majority of analyses from samples RT0776, RT07121 and  
279 BDW315A have  $\delta^{18}\text{O}$  values in the mantle range, but samples BDW315A and RT0678 have  
280  $\delta^{18}\text{O}$  values that are significantly lower than those from the mantle. Given the similar  $\epsilon_{\text{Hf}}(t)$   
281 values of these samples and the other northern Bemarivo Belt samples, we suggest that they  
282 were also generated from a juvenile depleted mantle source but involved hydrothermal fluids  
283 during magma generation. This may relate to their generation in an extensional environment  
284 (Bindeman and Valley, 2001; Valley et al., 1998). The felsic nature of the northern Bemarivo  
285 Belt suggests that the original magmas were likely to have fractionated in thickened crust. The  
286 juvenile Hf signatures of these samples, and mantle-like  $\delta^{18}\text{O}$  values, suggest that they formed  
287 in an arc environment, with little involvement of any significantly older, or supra-crustal  
288 material.

289 Our new Hf and O data from northern Madagascar indicate that the northern Bemarivo Belt  
290 and the southern Bemarivo Belt have very different isotopic evolutions and we therefore  
291 suggest that they were not contiguous at the time of their formation (c. 750 Ma). The Antsaba  
292 Shear Zone that marks the boundary between the northern and southern Bemarivo Belt  
293 (Thomas et al., 2009), also marks a boundary between samples of a juvenile signature in the  
294 north, and an evolved signature in the south. We therefore suggest that the Antsaba Shear  
295 Zone marks a major tectonic boundary in northern Madagascar and likely represents a cryptic  
296 suture zone.

## 297 **6 Assembly of north Malagasy Gondwana**

### 298 **6.1 Models for the assembly of northern Madagascar**

299 The terranes of northern Madagascar form a tectonically confusing triple-junction (Figure 1),  
300 with the southern Bemarivo Belt (including the Sahantaha Group), Anaboriana Belt and  
301 Antongil Domain all in contact with each other (Figure 1). We have shown here that rocks

302 from the Anaboriana Belt and southern Bemarivo Belt are isotopically similar, and we suggest  
303 that they were part of the same continental-margin volcanic arc system at c. 750 Ma. The  
304 relationship between these two terranes and the Antongil Domain, is less straightforward.  
305 Understanding the nature and timing of contacts between these three terranes is essential for  
306 understanding the evolution of northern Madagascar.

## 307 **6.2 The amalgamation of the Dharwar Craton with Madagascar**

308 The assembly of northern Madagascar is a contentious topic with different models proposed  
309 for the nature and timing of amalgamation (e.g. Armistead et al., 2017; Boger et al., 2014;  
310 Collins and Windley, 2002; Tucker et al., 2011). The relationship between the Sahantaha  
311 Group (maximum depositional age c. 1600 Ma, minimum depositional age c. 800 Ma) and the  
312 Antongil Craton provides clues as to the relative timing of these tectonic events. Despite the  
313 current fault contact marked by the major Andaparaty Thrust between the Sahantaha Group  
314 and Antongil Domain (Figure 1), several authors have suggested that the Sahantaha Group  
315 stratigraphically overlies the Antongil Domain (Bauer et al., 2011; De Waele et al., 2011),  
316 implying that the Antongil Domain must have been adjacent to central Madagascar at the  
317 time of deposition. Against this interpretation are the paucity of c. 3100 Ma detrital zircons in  
318 the Sahantaha Group (De Waele et al., 2008; Thomas et al., 2009), despite the Antongil  
319 Craton being rich in zircon-bearing protoliths of this age (Tucker et al., 1999b) and the lack of  
320 any depositional contact mapped between the terranes. We suggest that these observations  
321 support that the Sahantaha Group is allochthonous with respect to the Antongil Craton and  
322 that the two were juxtaposed by the major Andaparaty Thrust.

323 If these two terranes did form separately from each other, when did they come together?  
324 Widespread metamorphism throughout much of northern Madagascar is recorded at c. 530–  
325 510 Ma (Buchwaldt et al., 2003; Jöns et al., 2009), and we suggest that this event records the  
326 amalgamation of the Antongil Craton with the rest of Madagascar (including the Sahantaha  
327 Group and Anaboriana Belt), along the Betsimisaraka Suture of Collins and Windley (2002).

## 328 **6.3 What does the Anaboriana Belt represent?**

329 The Anaboriana-Manampotsy belt (Fig 1) has been interpreted to mark the approximate  
330 location of the Betsimisaraka Suture that has been interpreted as the site of amalgamation of  
331 the Antananarivo Craton with the Dharwar Craton (at the time including the Antongil-Masora  
332 domains) during the Ediacaran to early Cambrian (Armistead et al., 2017; Collins et al., 2003a;  
333 Collins and Windley, 2002). The Anaboriana Belt is the northern part of this extensive belt  
334 and separates the Sahantaha Group from the Antananarivo Craton. Above, we've argued that

335 the Sahantaha Group formed stratigraphically above the Antananarivo Craton, which implies  
336 that the Anaboriana Belt is not a suture, or at least would only have been a minor marginal  
337 Neoproterozoic ocean basin suture. An alternative interpretation for the Anaboriana-  
338 Manampotsy belt is that it does not represent a suture zone but was an elongated sedimentary  
339 basin that formed due to Tonian rifting (Tucker et al., 2011).

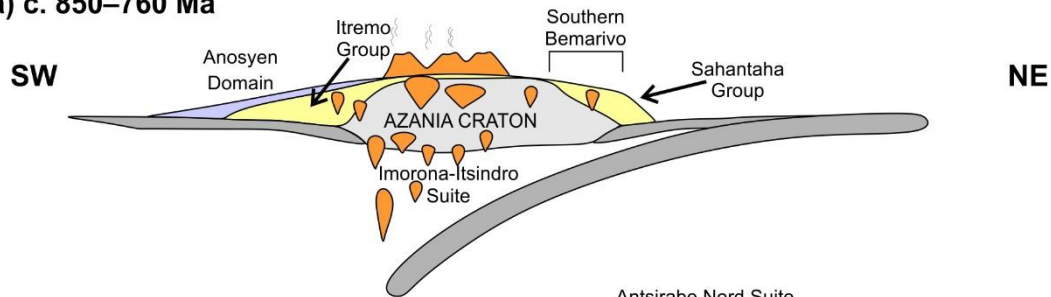
340 As we have described in our interpretation of samples from the Anaboriana Belt, due to  
341 pervasive high-grade metamorphism, it can be difficult to recognise sample protoliths as  
342 either sedimentary or magmatic in origin. It is therefore unclear whether the Anaboriana Belt  
343 represents a sedimentary sequence at all, or whether it should really be considered as a zone  
344 of major high-strain shearing. To date, samples from the entire length of the Anaboriana Belt  
345 have been interpreted with protolith ages ranging from c. 850 Ma to c. 750 Ma, with  
346 metamorphism interpreted from zircon rims at c. 550–520 Ma. Given the similarities in age  
347 and Hf isotope signatures between the Anaboriana Belt and the southern Bemarivo Belt, we  
348 suggest that the Anaboriana Belt was originally a c. 850–750 Ma group of rocks much like the  
349 southern Bemarivo Belt (and probably Imorona-Itsindro Suite) that were sheared and  
350 metamorphosed at c. 520 Ma, coinciding with emplacement of the age-equivalent Maevarano  
351 Suite. The more definitive metasedimentary rocks of the Manampotsy Belt to the south do  
352 demonstrate the presence of a Neoproterozoic basin in this area (Collins et al., 2003b). We  
353 suggest that this represents the Betsimisaraka Suture, but as it trends north, it becomes the  
354 Andaparaty Thrust, striking easterly into sea, and looping back on land as the Antsaba Shear  
355 Zone (Figure 1).

#### 356 **6.4 Final assembly of northern Madagascar**

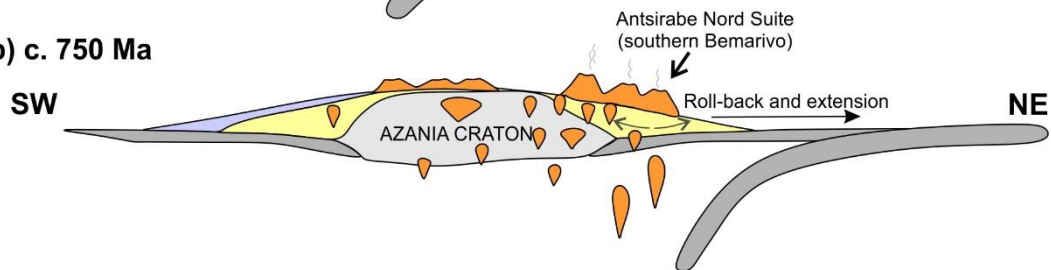
357 The c. 537–522 Ma Maevarano Suite (Goodenough et al., 2010) was previously interpreted to  
358 represent a maximum age constraint on the assembly of the Bemarivo Belt with the central  
359 Madagascar craton (Thomas et al., 2009). However, this was based on the premise that the  
360 Maevarano Suite intrusions were pervasive right throughout Madagascar—including the  
361 Bemarivo Belt—with the exception of the Antongil Craton. We have shown here that the  
362 northern and southern Bemarivo belts should be considered as two distinct terranes based on  
363 Hf and O isotopic differences, and therefore any interpretation of the Bemarivo Belt should  
364 consider these terranes separately. Despite geological mapping of Maevarano Suite granites in  
365 the northern Bemarivo Belt (BGS-USGS-GLW, 2008; Goodenough et al., 2010; Thomas et al.,  
366 2009), there are no published geochronological data to suggest that age equivalent Maevarano  
367 Suite granites are exposed here.

368 Similarly, the Maevarano Suite is not exposed in the Antongil Craton. The reasons given as to  
 369 why the Maevarano Suite does not crop out in the Antongil Craton were outlined by  
 370 Goodenough et al. (2010) and we suggest that these explanations are applicable to the  
 371 northern Bemarivo Belt. These are: 1) a suitable source was not present beneath these  
 372 terranes; and/or 2) structural controls led to the emplacement of magmas only in certain areas  
 373 (i.e. along shear zones). We suggest a third possibility for the northern Bemarivo Belt, where  
 374 this terrane may not have been accreted to Madagascar at the time of granite emplacement, or  
 375 that it was accreted in the very late stages of magmatism and therefore did not undergo the  
 376 same degree of crustal preconditioning. In any case, we suggest that the Maevarano Suite and  
 377 associated metamorphism, approximately marks the final assembly of northern Madagascar  
 378 into its current configuration.

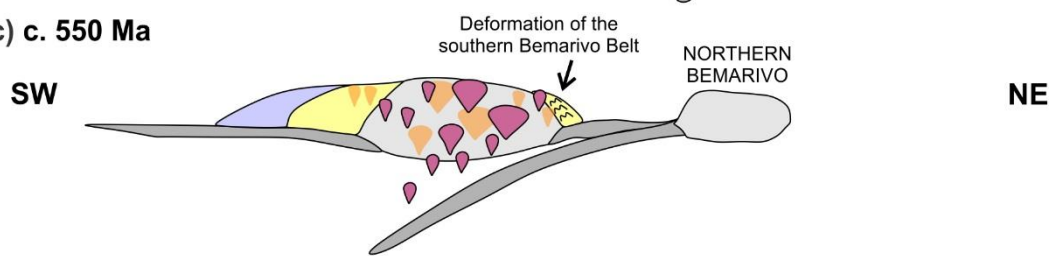
**a) c. 850–760 Ma**



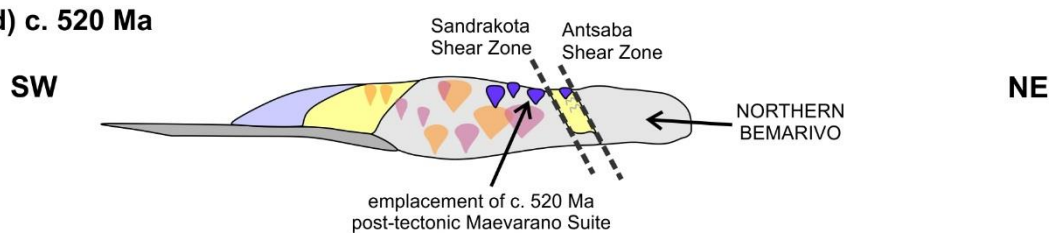
**b) c. 750 Ma**



**c) c. 550 Ma**



**d) c. 520 Ma**



379

380 Figure 5 Schematic diagram of the Neoproterozoic arc evolution of Madagascar. Part a modified after Boger  
381 et al. (2014). Features outlined in black (e.g. magmatic suites and fold belts) are active at that time period,  
382 grey outlined features are already emplaced.

## 383 7 Links to Rodinia

384 In an attempt to link the northern Bemarivo Belt with other potential c. 720 Ma arc terranes,  
385 we have compared our new isotopic data from the northern Bemarivo Belt with several regions  
386 containing age equivalent rocks. We compared the northern Bemarivo Belt with South China,  
387 northwest India, central Madagascar, Seychelles, Israel and the Arabian Nubian Shield (Figure  
388 6). We also integrated this dataset with the GPlates Neoproterozoic tectonic model (Merdith  
389 et al., 2017) to better assess correlations both temporally and spatially.

390 We have used a revised model of Merdith et al. (2017), which provides a framework for a  
391 global tectonic model during the Neoproterozoic. The benefit of using this model is that it  
392 takes into account paleogeographic constraints from other regions and integrates key datasets  
393 such as paleomagnetism, geochronology and geophysics to form a full-plate tectonic  
394 framework. We calculated an average age and average  $\epsilon_{\text{Hf}}(t)$  for each sample compiled in our  
395 database. This dataset was then added to GPlates as a shapefile and a start and end time for  
396 each data point was assigned  $\pm 30$  Ma (i.e. each point will show up 30 Ma before the average  
397 age and disappear 30 Ma after). Data points are coloured according to their average  $\epsilon_{\text{Hf}}(t)$   
398 value.

399 It has been suggested that the Imorona-Itsindro Suite of central Madagascar is analogous to  
400 the Seychelles and the Malani Igneous Suite granitoids based on age correlations (Tucker et  
401 al., 2001; Tucker et al., 2014). Tectonic models by Wang et al. (2017) and Ashwal et al. (2013)  
402 proposed a continuous juvenile Andean-type arc between south China, the Malani Igneous  
403 Suite of northwest India and Seychelles. Wang et al. (2017) further included the Imorona-  
404 Itsindro suite along with this magmatic arc. However, available  $\epsilon_{\text{Hf}}(t)$  data from the Imorona-  
405 Itsindro Suite of central Madagascar (Archibald et al., 2016; Zhou et al., 2018) is  
406 predominantly evolved (Figure 6), implying that it does not correlate with this juvenile arc  
407 system. Oman has also been interpreted as a series of arcs that accreted to Rajasthan in  
408 northwest India (which includes the Malani Igneous Suite) during the period c. 850–720 Ma  
409 (Blades et al., in review). We have shown here that age-equivalent rocks from the northern  
410 Bemarivo Belt, have juvenile  $\epsilon_{\text{Hf}}(t)$  signatures, which correlate well with  $\epsilon_{\text{Hf}}(t)$  data from the  
411 proposed south China–Malani–Seychelles arc system of Wang et al. (2017) as well as new data  
412 from Oman (Blades et al., in review) (Figure 6). These correlations are highlighted in the full-

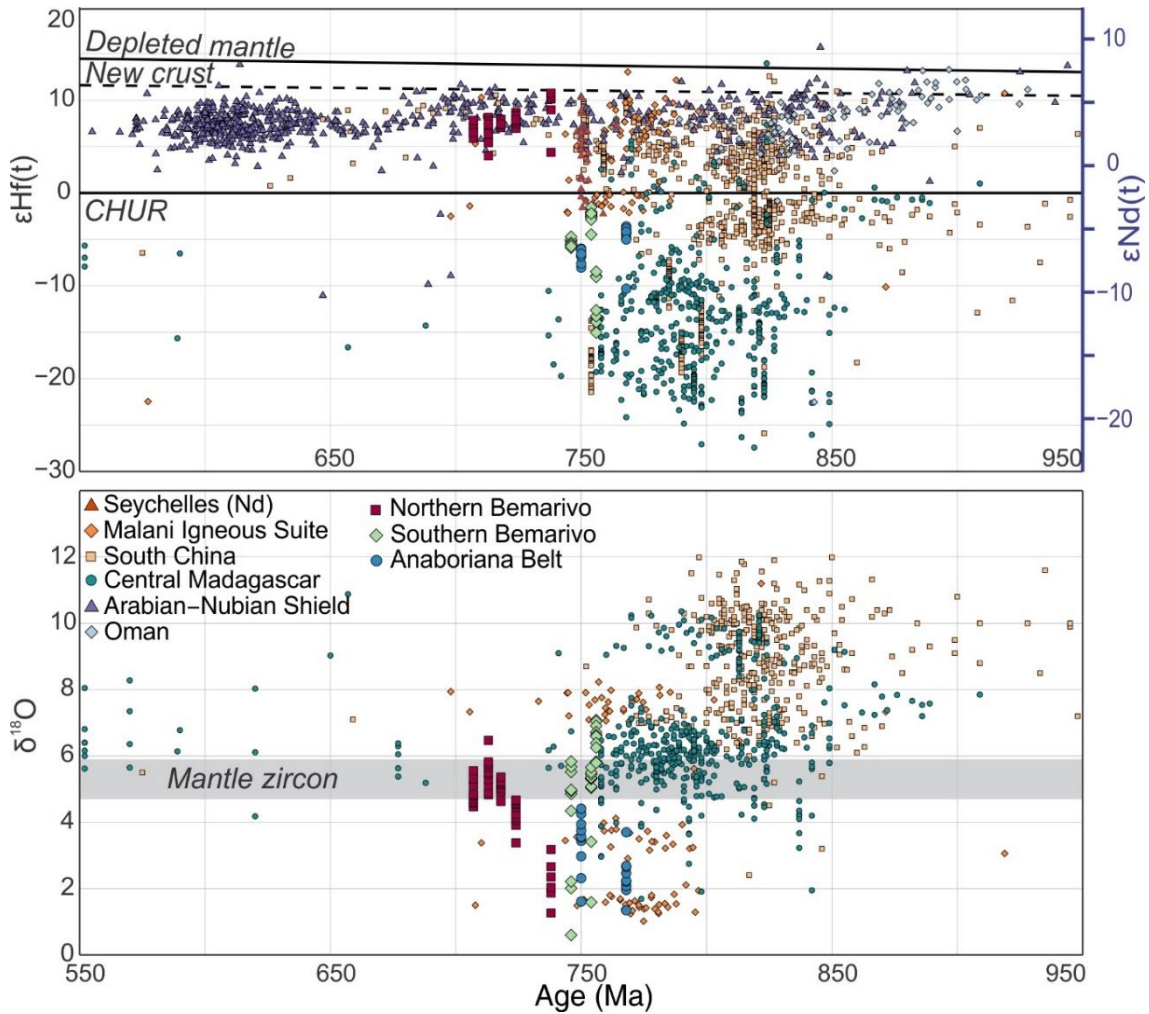
413 plate tectonic model in GPlates, where juvenile analyses (data points with shades of red;  
414 Figure 7) all form an elongated ‘arc’ along the western (reconstructed orientation) margin of  
415 India and China.

416 The period of arc magmatism in this proposed arc was long-lived, beginning at around c. 850  
417 Ma and ending at around c. 700 Ma. There is a general southward younging trend  
418 (reconstructed orientation; Figure 7), with the oldest record coming from China, and  
419 progressing to younger rocks through Oman, Malani, Seychelles and the northern Bemarivo  
420 Belt. It is possible that this period of juvenile arc magmatism represents a single long-lived arc,  
421 however, we suggest that a complex history of accretionary terranes that formed along the  
422 edge of Rodinia, is more likely.

423 Samples analysed from the northern Bemarivo Belt are slightly younger than rocks from south  
424 China and Malani, although they have similar juvenile  $\epsilon_{\text{Hf}}(t)$  signatures. It is therefore likely  
425 that the northern Bemarivo Belt formed during the late stages of this juvenile arc system,  
426 possibly on a rolled-back crustal remnant of south China, Malani or Oman-like crust. The  
427 whole-rock geochemistry data (Figure 4) suggest that the northern Bemarivo Belt underwent a  
428 degree of crustal assimilation and fractionation (see section 4). However, the  $\epsilon_{\text{Hf}}(t)$  data  
429 suggest that the northern Bemarivo Belt is dominantly juvenile, with little input of  
430 significantly older crustal material. Together this suggests that the crustal assimilate  
431 incorporated into magmatic rocks of the northern Bemarivo Belt was not significantly older  
432 than c. 720 Ma. This supports a model where the northern Bemarivo Belt formed on a crustal  
433 remnant of slightly older crust, possibly from south China, Malani or Oman (Alessio et al.,  
434 2018). This accounts for the crustal assimilation signatures in whole-rock geochemistry, and  
435 relatively juvenile  $\epsilon_{\text{Hf}}(t)$  signatures.

436 The integration of  $\epsilon_{\text{Hf}}(t)$  data with the full-plate tectonic model of (Merdith et al., 2017)  
437 broadly supports the south China–Malani–Seychelles linkage proposed by Wang et al. (2017)  
438 and Ashwal et al. (2013), and the links between Oman and northwest India proposed by  
439 Blades et al. (in review). We further extend this model to include the northern Bemarivo Belt  
440 of northern Madagascar as a younger, more outboard component of this arc system. There is  
441 no significant overlap between the highly evolved data from the Imorona-Itsindro Suite and  
442 that of this proposed Neoproterozoic arc system. The lack of juvenile Hf data from the  
443 Imorona-Itsindro Suite suggests that this terrane was not part of the south China–Malani–  
444 Seychelles–Bemarivo arc, which is dominated by weakly evolved to juvenile rocks.

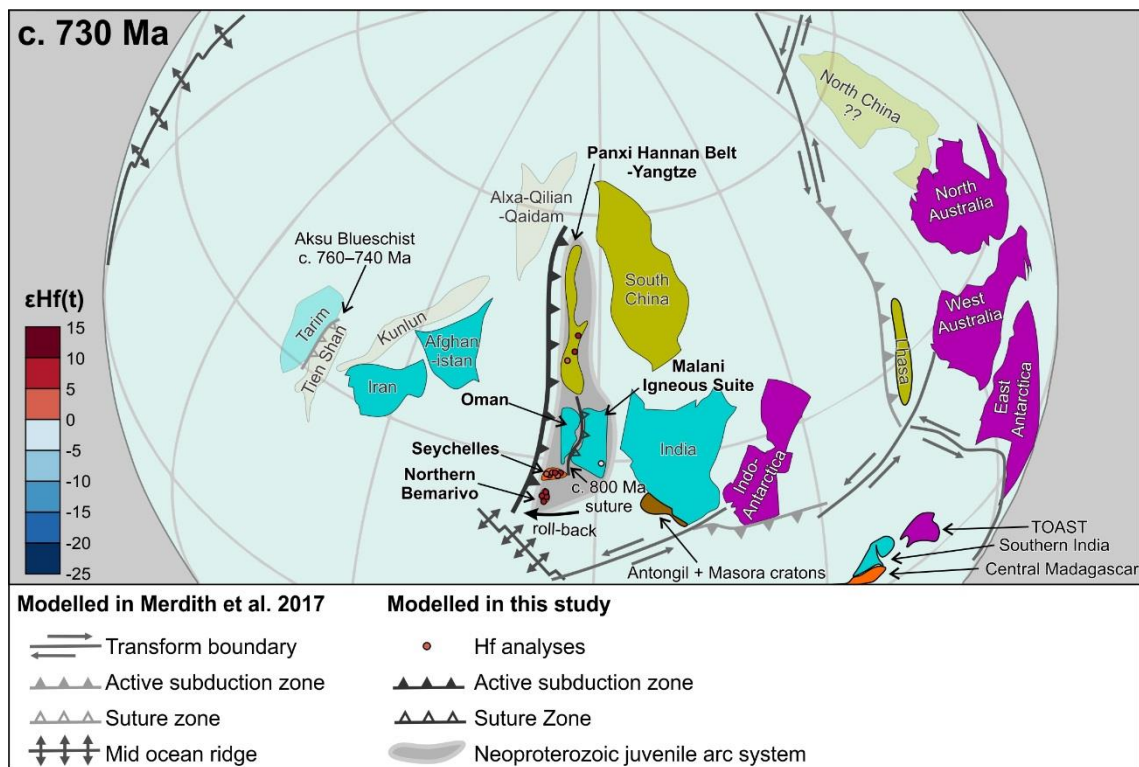
445 Our proposal of linking these previously discrete volcanic arcs into a long-lived subduction  
 446 zone can help elucidate long term trends in plate boundary length and, when compared to the  
 447 connectedness of continental lithosphere, assist with quantitatively understanding the  
 448 supercontinent cycle for pre-Pangea supercontinents (e.g. Meredith et al., in review). We have  
 449 shown the power of integrating big isotopic data compilations into a plate tectonics  
 450 framework to better understand the evolution of supercontinents through time.



451

452 Figure 6  $\epsilon_{\text{Hf}}(t)$  vs age and  $\delta^{18}\text{O}$  vs age for other regions compared to northern Madagascar; Seychelles data is  
 453 converted from  $\epsilon_{\text{Nd}}(t)$  to  $\epsilon_{\text{Hf}}(t)$  using the equation  $\epsilon_{\text{Hf}}(t) = 1.34\epsilon_{\text{Nd}}(t) + 2.95$  for 'terrestrial array' (Vervoort et  
 454 al., 1999) and scale is shown to the right of the plot. R scripts to produce plots are provided in supplementary  
 455 file C. Data sourced from: Alessio et al. (2018); Archibald et al. (2016); Ashwal et al. (2002); Blades et al.  
 456 (2015); Huang et al. (2008); Long et al. (2011); Morag et al. (2011); Qi et al. (2012); Robinson et al. (2014);  
 457 Wang et al. (2017); Wang et al. (2013); Zhao et al. (2013); Zheng et al. (2008); Zheng et al. (2007); Zhou et al.  
 458 (2018).

459



460

461 Figure 7 GPlates reconstruction at 730 Ma showing the location of compiled Hf and Nd isotope data (see  
 462 Figure 6 for the conversion calculation used). Transparent polygons are uncertain in the model but are  
 463 included as suggestions based on their positions post-Gondwana amalgamation. Lhasa is linked to Australia  
 464 after Zhu et al. (2011), addition of the TOAST terrane to Azania after Jacobs et al. (2015) and Archibald et al.  
 465 (2017a).

## 466 8 Conclusions

467 We have presented new zircon Hf and O isotope data that help unravel the subduction history  
 468 of the Mozambique Ocean during the critical time of supercontinent cycle transition—from  
 469 the Nuna/Rodinia cycle to the amalgamation of Gondwana. We have compared these  
 470 Madagascar data to other age-equivalent terranes globally. The key outcomes of this research  
 471 are:

- 472 1. The northern and southern Bemarivo belts are different terranes that have separate  
 473 tectonic evolutions until the Cambrian, based on zircon  $\epsilon_{\text{Hf}}(t)$  and  $\delta^{18}\text{O}$  data.

- 474 2. The c. 750 Ma southern Bemarivo Belt and Anaboriana Belt are isotopically evolved  
475 terranes that may represent a younger component of the retreating volcanic arc  
476 represented in central Madagascar by the Imorona-Itsindro Suite.
- 477 3. The c. 720 Ma northern Bemarivo Belt is a juvenile terrane that we suggest formed in a  
478 juvenile arc environment related to the Seychelles, the Malani Igneous Suite of  
479 northwest India, Oman and the Yangtze Belt of South China. This is interpreted as  
480 formation above an aging, retreating, subduction zone.
- 481 4. The northern Bemarivo Belt collided with Madagascar at c. 520 Ma, after the main  
482 phase of orogenesis produced by the Betsimisaraka Suture.

## 483 **9 Acknowledgements**

484 Peter Holden is thanked for assistance with O isotope data collection and processing. The  
485 University of Adelaide TRaX research group are thanked for their continued support and  
486 collaboration. Raisa Lopes Costa is thanked for the use of a digitised geological map of  
487 Madagascar (fig 1). The British Geological Survey are thanked for the use of zircon mounts  
488 produced through the Madagascar World Bank Project. SA is funded by an Australian  
489 government PhD Scholarship and AC is funded by an Australian Research Council Future  
490 Fellowship FT120100340. This forms TRaX Record XX and is a contribution to IGCP projects  
491 628 (Gondwana Map) and 648 (Supercontinent Cycles and Global Geodynamics). We thank  
492 the reviewers for their helpful feedback on this manuscript.

493 Table 1: Summary of samples and U–Pb zircon geochronology used in this study. All ages are interpreted as magmatic crystallisation ages, except for those indicated by \*  
 494 which are interpreted as maximum depositional ages, and ^ which are interpreted as metamorphic ages. Generally, for samples with lots of concordant analyses we used  
 495 a cut-off of  $\pm 5\%$  concordance.

Sample	Longitude (WGS 84)	Latitude (WGS 84)	Region	Stratigraphic unit or domain	Rock description	$^{238}\text{U}/^{206}\text{Pb}$ Age (Ma) $\pm 2\sigma$	Calculation method
RK7219	48.9828	-15.1957	Anaboriana-Manampotsy belt	Groupe d'Androna-Manampotsy	Quartzofeldspathic gneiss	750 $\pm$ 4 *573 $\pm$ 13 ^514 $\pm$ 6	Weighted average of oldest near-concordant analyses: n=8, MSWD=0.80 *Youngest near-concordant (within 5%) zircon core analysis ^Metamorphic age: n=4, MSWD=0.93
BT0751	48.6479	-14.5132	Anaboriana-Manampotsy belt	Group de Bealanana, Anaboriana belt	Charnockite gneiss	768 $\pm$ 8 *561 $\pm$ 8 ^518 $\pm$ 4	Weighted average of oldest near-concordant analyses: n= 6, MSWD=1.4 *Youngest near-concordant (within 5%) zircon core analysis ^Metamorphic age: n=7, MSWD=0.59
RT06467	49.7379	-14.2695	Southern Bemarivo Domain	Bemarivo Domain	Granodioritic gneiss	756 $\pm$ 6	n=14, MSWD=0.60
BT0641	49.9411	-14.0582	Southern Bemarivo Domain	Doany Arc, Bemarivo Domain	Tonalitic orthogneiss	746 $\pm$ 4	n=13, MSWD=1.5
BT06_36	49.9153	-13.9953	Southern Bemarivo Domain	Antsirabe-North Suite, Douany arc, Bemarivo Block	Diorite	754 $\pm$ 7	n=12, MSWD=0.69
RT0776	49.4385	-13.4362	Northern Bemarivo Domain	Bevoay Massif	Mica Granite	713 $\pm$ 6	n=5, MSWD=0.63
RT07121	48.7316	-13.7815	Northern Bemarivo Domain	Bemarivo Domain	Metagranodiorite gneiss	707 $\pm$ 5	n=6, MSWD=2.0
BDW315A	49.3712	-13.766	Northern Bemarivo Domain	Bemarivo Domain	Metagranodiorite	718 $\pm$ 7	n=6, MSWD=0.38
BB06A12	49.8762	-13.2988	Northern Bemarivo Domain	Daraina Group	Metarhyolite – flow banded	724 $\pm$ 7	n=9, MSWD=0.98
RT0678	49.741	-12.9375	Northern Bemarivo Domain	Daraina Group	Rhyolite	738 $\pm$ 7	n=5, MSWD=1.2

496

## 10 References

- 498 Alessio, B.L., Blades, M.L., Murray, G., Thorpe, B., Collins, A.S., Kelsey, D.E., Foden, J., Payne, J., Al-Khirbash, S. and  
 499 Jourdan, F., 2018. Origin and tectonic evolution of the NE basement of Oman: a window into the  
 500 Neoproterozoic accretionary growth of India? *Geological Magazine*, 155(5): 1150-1174.
- 501 Archibald, D.B., Collins, A.S., Foden, J.D., Payne, J.L., Holden, P., Razakamanana, T., De Waele, B., Thomas, R.J. and  
 502 Pitfield, P.E.J., 2016. Genesis of the Tonian Imorona-Itsindro magmatic Suite in central Madagascar:  
 503 Insights from U-Pb, oxygen and hafnium isotopes in zircon. *Precambrian Research*, 281: 312-337.
- 504 Archibald, D.B., Collins, A.S., Foden, J.D., Payne, J.L., Macey, P.H., Holden, P. and Razakamanana, T., 2017a.  
 505 Stenian-Tonian arc magmatism in west-central Madagascar: the genesis of the Dabolava Suite. *Journal of*  
 506 *the Geological Society*: jgs2017-028.
- 507 Archibald, D.B., Collins, A.S., Foden, J.D. and Razakamanana, T., 2017b. Tonian Arc Magmatism in Central  
 508 Madagascar: The Petrogenesis of the Imorona-Itsindro Suite. *The Journal of Geology*, 125(3): 000-000.
- 509 Armistead, S.E., Collins, A.S., Payne, J.L., Foden, J.D., De Waele, B., Shaji, E. and Santosh, M., 2017. A re-evaluation  
 510 of the Kumta Suture in western peninsular India and its extension into Madagascar. *Journal of Asian Earth*  
 511 *Sciences*.
- 512 Ashwal, L., Demaiffe, D. and Torsvik, T., 2002. Petrogenesis of Neoproterozoic granitoids and related rocks from  
 513 the Seychelles: the case for an Andean-type arc origin. *Journal of Petrology*, 43(1): 45-83.
- 514 Ashwal, L.D., Solanki, A.M., Pandit, M.K., Corfu, F., Hendriks, B.W.H., Burke, K. and Torsvik, T.H., 2013.  
 515 Geochronology and geochemistry of Neoproterozoic Mt. Abu granitoids, NW India: Regional correlation  
 516 and implications for Rodinia paleogeography. *Precambrian Research*, 236: 265-281.
- 517 Bauer, W., Walsh, G.J., de Waele, B., Thomas, R.J., Horstwood, M.S.A., Bracciali, L., Schofield, D.I., Wollenberg, U.,  
 518 Lidke, D.J., Rasaona, I.T. and Rabarimanana, M.H., 2011. Cover sequences at the northern margin of the  
 519 Antongil Craton, NE Madagascar. *Precambrian Research*, 189(3-4): 292-312.
- 520 BGS-USGS-GLW, 2008. Republique de Madagascar Ministère de L'energie et des Mines  
 521 (MEM/SG/DG/UCP/PGRM). British Geological Survey Research Report.
- 522 Bindeman, I.N. and Valley, J.W., 2001. Low- $\delta^{18}\text{O}$  rhyolites from Yellowstone: Magmatic evolution based on  
 523 analyses of zircons and individual phenocrysts. *Journal of Petrology*, 42(8): 1491-1517.
- 524 Blades, M.L., Collins, A.S., Foden, J., Payne, J.L., Xu, X., Alemu, T., Woldetinsae, G., Clark, C. and Taylor, R.J.M.,  
 525 2015. Age and hafnium isotopic evolution of the Didesa and Kemashi Domains, western Ethiopia.  
 526 *Precambrian Research*, 270: 267-284.
- 527 Boger, S.D., Hirdes, W., Ferreira, C.A.M., Schulte, B., Jenett, T. and Fanning, C.M., 2014. From passive margin to  
 528 volcano-sedimentary forearc: The Tonian to Cryogenian evolution of the Anosyen Domain of  
 529 southeastern Madagascar. *Precambrian Research*, 247: 159-186.
- 530 Buchwaldt, R., Tucker, R.D. and Dymek, R.F., 2003. Geothermobarometry and U-Pb Geochronology of metapelitic  
 531 granulites and pelitic migmatites from the Lokoho region, Northern Madagascar. *American Mineralogist*,  
 532 88(11-12): 1753-1768.
- 533 Collins, A.S., 2006. Madagascar and the amalgamation of Central Gondwana. *Gondwana Research*, 9(1-2): 3-16.
- 534 Collins, A.S., Fitzsimons, I.C.W., Hulscher, B. and Razakamanana, T., 2003a. Structure of the eastern margin of the  
 535 East African Orogen in central Madagascar. *Precambrian Research*, 123(2-4): 111-133.
- 536 Collins, A.S., Kröner, A., Fitzsimons, I.C.W. and Razakamanana, T., 2003b. Detrital footprint of the Mozambique  
 537 ocean: U-Pb SHRIMP and Pb evaporation zircon geochronology of metasedimentary gneisses in eastern  
 538 Madagascar. *Tectonophysics*, 375(1-4): 77-99.
- 539 Collins, A.S. and Pisarevsky, S.A., 2005. Amalgamating eastern Gondwana: The evolution of the Circum-Indian  
 540 Orogens. *Earth-Science Reviews*, 71(3-4): 229-270.
- 541 Collins, A.S. and Windley, B.F., 2002. The tectonic evolution of central and northern Madagascar and its place in  
 542 the final assembly of Gondwana. *The Journal of geology*, 110(3): 325-339.
- 543 Condie, K.C., 2002. Breakup of a Paleoproterozoic supercontinent. *Gondwana Research*, 5(1): 41-43.
- 544 Cox, R., Armstrong, R.A. and Ashwal, L.D., 1998. Sedimentology, geochronology and provenance of the Proterozoic  
 545 Itremo Group, central Madagascar, and implications for pre-Gondwana palaeogeography. *Journal of the*  
 546 *Geological Society*, 155(6): 1009-1024.
- 547 Cox, R., Coleman, D.S., Chokel, C.B., DeOreo, S.B., Wooden, J.L., Collins, A.S., De Waele, B. and Kröner, A., 2004.  
 548 Proterozoic Tectonostratigraphy and Paleogeography of Central Madagascar Derived from Detrital Zircon  
 549 U-Pb Age Populations. *The Journal of geology*, 112(4): 379-399.
- 550 De Waele, B., Thomas, R.J., Horstwood, M., Pitfield, P., Tucker, R., Potter, C., Key, R., Smith, R., Bauer, W. and  
 551 Randriamananjara, T., 2008. U-Pb detrital zircon geochronological provenance patterns of supracrustal  
 552 successions in central and northern Madagascar.
- 553 De Waele, B., Thomas, R.J., Macey, P.H., Horstwood, M.S.A., Tucker, R.D., Pitfield, P.E.J., Schofield, D.I.,  
 554 Goodenough, K.M., Bauer, W., Key, R.M., Potter, C.J., Armstrong, R.A., Miller, J.A., Randriamananjara, T.,  
 555 Ralison, V., Rafahatelo, J.M., Rabarimanana, M. and Bejoma, M., 2011. Provenance and tectonic

556 significance of the Palaeoproterozoic metasedimentary successions of central and northern Madagascar.  
557 Precambrian Research, 189(1-2): 18-42.

558 Emmel, B., Jons, N., Kroner, A., Jacobs, J., Wartho, J.A., Schenk, V., Razakamanana, T. and Austegard, A., 2008.  
559 From Closure of the Mozambique Ocean to Gondwana Breakup: New Evidence from Geochronological  
560 Data of the Vohibory Terrane, Southwest Madagascar. *The Journal of Geology*, 116(1): 21-38.

561 Fernandez, A., Schreurs, G., Villa, I.M., Huber, S. and Rakotondrazafy, M., 2003. Age constraints on the tectonic  
562 evolution of the Itremo region in Central Madagascar. *Precambrian Research*, 123(2-4): 87-110.

563 Fitzsimons, I.C.W. and Hulscher, B., 2005. Out of Africa: detrital zircon provenance of central Madagascar and  
564 Neoproterozoic terrane transfer across the Mozambique Ocean. *Terra Nova*, 17(3): 224-235.

565 Fritz, H., Abdelsalam, M., Ali, K.A., Bingen, B., Collins, A.S., Fowler, A.R., Ghebreab, W., Hauzenberger, C.A.,  
566 Johnson, P.R., Kusky, T.M., Macey, P., Muhongo, S., Stern, R.J. and Viola, G., 2013. Orogen styles in the  
567 East African Orogen: A review of the Neoproterozoic to Cambrian tectonic evolution. *Journal of African  
568 Earth Sciences*, 86: 65-106.

569 Frost, B.R. and Frost, C.D., 2008. A geochemical classification for feldspathic igneous rocks. *Journal of Petrology*,  
570 49(11): 1955-1969.

571 Goodenough, K.M., Thomas, R.J., De Waele, B., Key, R.M., Schofield, D.I., Bauer, W., Tucker, R.D., Rafahatelo, J.M.,  
572 Rabarimanana, M., Ralison, A.V. and Randriamananjara, T., 2010. Post-collisional magmatism in the  
573 central East African Orogen: The Maevarano Suite of north Madagascar. *Lithos*, 116(1-2): 18-34.

574 Huang, X.-L., Xu, Y.-G., Li, X.-H., Li, W.-X., Lan, J.-B., Zhang, H.-H., Liu, Y.-S., Wang, Y.-B., Li, H.-Y. and Luo, Z.-Y.,  
575 2008. Petrogenesis and tectonic implications of Neoproterozoic, highly fractionated A-type granites from  
576 Mianning, South China. *Precambrian Research*, 165(3-4): 190-204.

577 Jacobs, J., Elburg, M., Läufer, A., Kleinhanns, I.C., Henjes-Kunst, F., Estrada, S., Ruppel, A.S., Damaske, D.,  
578 Montero, P. and Bea, F., 2015. Two distinct late Mesoproterozoic/early Neoproterozoic basement  
579 provinces in central/eastern Dronning Maud Land, East Antarctica: The missing link, 15–21 E.  
580 *Precambrian Research*, 265: 249-272.

581 Jöns, N., Emmel, B., Schenk, V. and Razakamanana, T., 2009. From orogenesis to passive margin—the cooling  
582 history of the Bemarivo Belt (N Madagascar), a multi-thermochronometer approach. *Gondwana Research*,  
583 16(1): 72-81.

584 Jöns, N. and Schenk, V., 2007. Relics of the Mozambique Ocean in the central East African Orogen: evidence from  
585 the Vohibory Block of southern Madagascar. *Journal of Metamorphic Geology*, 0(0): 071115150845002-  
586 ???

587 Kröner, A., Hegner, E., Collins, A.S., Windley, B.F., Brewer, T.S., Razakamanana, T. and Pidgeon, R.T., 2000. Age  
588 and magmatic history of the Antananarivo Block, central Madagascar, as derived from zircon  
589 geochronology and Nd isotopic systematics. *American Journal of Science*, 300(4): 251-288.

590 Long, X., Yuan, C., Sun, M., Kröner, A., Zhao, G., Wilde, S. and Hu, A., 2011. Reworking of the Tarim Craton by  
591 underplating of mantle plume-derived magmas: evidence from Neoproterozoic granitoids in the  
592 Kuluketage area, NW China. *Precambrian Research*, 187(1-2): 1-14.

593 Mallard, C., Coltice, N., Seton, M., Müller, R.D. and Tackley, P.J., 2016. Subduction controls the distribution and  
594 fragmentation of Earth's tectonic plates. *Nature*, 535(7610): 140.

595 Merdith, A.S., Collins, A.S., Williams, S.E., Pisarevsky, S., Foden, J.D., Archibald, D.B., Blades, M.L., Alessio, B.L.,  
596 Armistead, S. and Plavsa, D., 2017. A full-plate global reconstruction of the Neoproterozoic. *Gondwana  
597 Research*, 50: 84-134.

598 Morag, N., Avigad, D., Gerdes, A., Belousova, E. and Harlavan, Y., 2011. Crustal evolution and recycling in the  
599 northern Arabian-Nubian Shield: New perspectives from zircon Lu–Hf and U–Pb systematics.  
600 *Precambrian Research*, 186(1-4): 101-116.

601 Nance, R.D., Murphy, J.B. and Santosh, M., 2014. The supercontinent cycle: a retrospective essay. *Gondwana  
602 Research*, 25(1): 4-29.

603 Qi, X., Zeng, L., Zhu, L., Hu, Z. and Hou, K., 2012. Zircon U–Pb and Lu–Hf isotopic systematics of the Daping  
604 plutonic rocks: implications for the Neoproterozoic tectonic evolution of the northeastern margin of the  
605 Indochina block, Southwest China. *Gondwana Research*, 21(1): 180-193.

606 Robinson, F.A., Foden, J.D., Collins, A.S. and Payne, J.L., 2014. Arabian Shield magmatic cycles and their  
607 relationship with Gondwana assembly: Insights from zircon U–Pb and Hf isotopes. *Earth and Planetary  
608 Science Letters*, 408: 207-225.

609 Roig, J., Tucker, R., Delor, C., Peters, S. and Théveniaut, H., 2012. Carte géologique de la République de  
610 Madagascar à 1/1 000 000. Ministère des Mines, PGRM, Antananarivo, République de Madagascar, 1.

611 Schofield, D.I., Thomas, R.J., Goodenough, K.M., De Waele, B., Pitfield, P.E.J., Key, R.M., Bauer, W., Walsh, G.J.,  
612 Lidke, D.J. and Ralison, A.V., 2010. Geological evolution of the Antongil Craton, NE Madagascar.  
613 *Precambrian Research*, 182(3): 187-203.

614 Sun, S.-S. and McDonough, W.-S., 1989. Chemical and isotopic systematics of oceanic basalts: implications for  
615 mantle composition and processes. *Geological Society, London, Special Publications*, 42(1): 313-345.

616 Thomas, R.J., De Waele, B., Schofield, D.I., Goodenough, K.M., Horstwood, M., Tucker, R., Bauer, W., Annells, R.,  
617 Howard, K., Walsh, G., Rabarimanana, M., Rafahatelo, J.M., Ralison, A.V. and Randriamananjara, T., 2009.

618 Geological evolution of the Neoproterozoic Bemarivo Belt, northern Madagascar. *Precambrian Research*,  
619 172(3-4): 279-300.

620 Tucker, R., Ashwal, L., Hamilton, M., Torsvik, T. and Carter, L., 1999a. Neoproterozoic silicic magmatism of  
621 northern Madagascar, Seychelles, and NW India: clues to Rodinia's assembly and dispersal, *Geological*  
622 *Society of America, Abstracts with Programs*, pp. 317.

623 Tucker, R., Ashwal, L., Handke, M., Hamilton, M., Le Grange, M. and Rambeloson, R., 1999b. U-Pb geochronology  
624 and isotope geochemistry of the Archean and Proterozoic rocks of north-central Madagascar. *The Journal*  
625 *of Geology*, 107(2): 135-153.

626 Tucker, R., Ashwal, L. and Torsvik, T., 2001. U-Pb geochronology of Seychelles granitoids: a Neoproterozoic  
627 continental arc fragment. *Earth and Planetary Science Letters*, 187(1-2): 27-38.

628 Tucker, R., Roig, J.-Y., Delor, C., Amelin, Y., Goncalves, P., Rabarimanana, M., Ralison, A. and Belcher, R., 2011.  
629 Neoproterozoic extension in the Greater Dharwar Craton: a reevaluation of the "Betsimisaraka suture" in  
630 Madagascar. *Canadian Journal of Earth Sciences*, 48(2): 389-417.

631 Tucker, R.D., Roig, J.Y., Moine, B., Delor, C. and Peters, S.G., 2014. A geological synthesis of the Precambrian shield  
632 in Madagascar. *Journal of African Earth Sciences*, 94: 9-30.

633 Valley, J.W., Kinny, P.D., Schulze, D.J. and Spicuzza, M.J., 1998. Zircon megacrysts from kimberlite: oxygen isotope  
634 variability among mantle melts. *Contributions to mineralogy and petrology*, 133(1-2): 1-11.

635 Vervoort, J.D., Patchett, P.J., Blichert-Toft, J. and Albarède, F., 1999. Relationships between Lu-Hf and Sm-Nd  
636 isotopic systems in the global sedimentary system. *Earth and Planetary Science Letters*, 168(1): 79-99.

637 Wang, W., Cawood, P.A., Zhou, M.F., Pandit, M.K., Xia, X.P. and Zhao, J.H., 2017. Low- $\delta^{18}\text{O}$  Rhyolites From the  
638 Malani Igneous Suite: A Positive Test for South China and NW India Linkage in Rodinia. *Geophysical*  
639 *Research Letters*, 44(20).

640 Wang, Y., Zhang, A., Cawood, P.A., Fan, W., Xu, J., Zhang, G. and Zhang, Y., 2013. Geochronological, geochemical  
641 and Nd-Hf-Os isotopic fingerprinting of an early Neoproterozoic arc-back-arc system in South China and  
642 its accretionary assembly along the margin of Rodinia. *Precambrian Research*, 231: 343-371.

643 Zhao, J.-H., Zhou, M.-F. and Zheng, J.-P., 2013. Constraints from zircon U-Pb ages, O and Hf isotopic compositions  
644 on the origin of Neoproterozoic peraluminous granitoids from the Jiangnan Fold Belt, South China.  
645 *Contributions to Mineralogy and Petrology*, 166(5): 1505-1519.

646 Zheng, Y.-F., Wu, R.-X., Wu, Y.-B., Zhang, S.-B., Yuan, H. and Wu, F.-Y., 2008. Rift melting of juvenile arc-derived  
647 crust: geochemical evidence from Neoproterozoic volcanic and granitic rocks in the Jiangnan Orogen,  
648 South China. *Precambrian Research*, 163(3): 351-383.

649 Zheng, Y.-F., Zhang, S.-B., Zhao, Z.-F., Wu, Y.-B., Li, X., Li, Z. and Wu, F.-Y., 2007. Contrasting zircon Hf and O  
650 isotopes in the two episodes of Neoproterozoic granitoids in South China: implications for growth and  
651 reworking of continental crust. *Lithos*, 96(1-2): 127-150.

652 Zhou, J.-L., Li, X.-H., Tang, G.-Q., Liu, Y. and Tucker, R.D., 2018. New evidence for a continental rift tectonic  
653 setting of the Neoproterozoic Imorona-Itsindro Suite (central Madagascar). *Precambrian Research*, 306:  
654 94-111.

655 Zhu, D.-C., Zhao, Z.-D., Niu, Y., Dilek, Y. and Mo, X.-X., 2011. Lhasa terrane in southern Tibet came from Australia.  
656 *Geology*, 39(8): 727-730.

657